Geomorphology 121 (2010) 55–68

Contents lists available at ScienceDirect

Geomorphology

journal homepage: www.elsevier.com/locate/geomorph

Long-time evolution of models of aeolian sand dune fields: Influence of dune formation and collision

Serina Diniega [a,*], Karl Glasner [b], Shane Byrne [c]

[a] Program in Applied Mathematics, The University of Arizona, 617 N. Santa Rita Ave., P.O. Box 210089, Tucson, AZ, 5 85721-0089, USA
[b] Department of Mathematics, University of Arizona, USA
[c] Department of Planetary Sciences, University of Arizona, USA

ARTICLE INFO

Article history:
Received 18 July 2008
Received in revised form 8 December 2008
Accepted 6 February 2009
Available online 20 February 2009

Keywords:
Sand dune
Dune field
Dune field model
Dune collision
Coarsening
Coalescence

ABSTRACT

Theoretical models which approximate individual sand dunes as particles that move and interact via simple rules are currently the only viable method for examining whether large dune fields will evolve into a patterned structure. We find that these types of simulations are sensitive to the influx condition and interaction function, and are not necessarily robust under common assumptions. In this paper, we review continuum dune models and how they connect to models of dune fields that approximate dunes as interacting particles with collision and coalescence dynamics. This type of simple dune field model is examined under different boundary and initial conditions. We identify different long-term behaviors depending on model parameters as well as the way in which dunes are initialized and collide. A "rule" for predicting the end state of a modelled dune field is derived, based on the statistics of a uniform influx dune size distribution and the interaction function. Possible future adjustments to the multiscale model, such as the use of a Gaussian influx dune size distribution, and their effect on the prediction rule are also discussed.

1. Introduction

Many dune fields appear to exhibit regular patterns (Bishop, 2007), indicating they may evolve through a process of self-organization (Werner, 1995; Kocurek and Ewing, 2005). Continuum dune models which examine the evolution of one or a few dunes, however, show that individual dunes are unstable with respect to changes in the sand flux, which implies that dunes in a field, evolving only through sand flux, should eventually coalesce into a small number of large dunes (Hersen et al., 2004). Thus, steady-state fields of similarly sized and size-limited dunes should not form, unless other stabilizing processes are also at work. For example, variations in wind strength and direction can destabilize large dunes and may play a major role for size selection in dune fields (Elbelrhiti et al., 2005). However, such processes are often stochastic or dependent strongly on local environmental conditions, and, thus, are difficult to incorporate into generic analysis or simulation of dune fields.

One mechanism that has been proposed to regulate dune size and spacing, and that depends on sand and dune dynamics broadly common to all dune fields, is dune collision. When dunes collide, sand is redistributed between the dunes. As long as the net sand exchange is from the large to the small dune, it would be possible for a dune field to evolve into a patterned structure after many collisions (Hersen and Douady, 2005). To evaluate this premise, one might consider applying a continuum model to a field consisting of hundreds of dunes. Because of the large temporal and spatial scales involved and current technology limitations, however, this is not feasible.

To understand how a dune field evolves through collisions, a multiscale approach is needed. This involves using a continuum model to investigate the evolution of single dunes and the interaction of two (or a few) dunes. The large scale model is then constructed by regarding dunes as particles, and using the continuum model results to construct phenomenological rules to prescribe the motion and interaction of the particles.

Various studies of transverse (Parteli and Herrmann, 2003; Lee et al., 2005) and barchan (Lima et al., 2002) dune fields have utilized this type of approach. These studies make predictions about dune spacing and size trends, and compare results with observed dune fields. Our purpose here is to generalize these models to determine how robust the conclusions are.

The results of this study will: (i) aid dune field modelers as they design their models, (ii) aid planetary scientists and geologists in better interpreting the results of dune field models by helping them understand how structural elements can (perhaps unintentionally) influence results, and (iii) emphasize that more observational and experimental data about dune formation and interaction is needed to help constrain/calibrate dune field models.

This paper consists of two parts: we first describe how to build a multiscale model by using a continuum dune model (Section 2.1, 2.2) to examine the effects of dune collisions (Sections 2.3, 2.4). Compiling

* Corresponding author. Tel.: +1 520 326 0481; fax: +1 520 626 5048.
E-mail addresses: serina@math.arizona.edu (S. Diniega), kglasner@math.arizona.edu (K. Glasner), shane@lpl.arizona.edu (S. Byrne).

0169-555X/$ – see front matter © 2009 Elsevier B.V. All rights reserved.
doi:10.1016/j.geomorph.2009.02.010

the results of many dune collision simulations, we create an interaction function to predict the results of any dune collision from the sizes of the colliding dunes. Although the derived interaction function yields only coalescence-dominated dynamics (Section 2.5), its construction and overall form serves as the basis of how a generic interaction function should appear. Finally, we define the various assumptions and parameters which go into our collision-dynamics dune field model (Section 3).

In the second part of this paper, we first outline the different outcomes of dune field models (Section 4.1). We then test for the influence that various components of a dune field model have on those outcomes: exact interaction function form (Section 4.2), boundary type (Section 4.3), and initial/influx conditions (Section 4.4). After identifying the two important parameters, a statistical analysis of the probability that any single interaction will result in more similarly sized dunes yields predictions about whether a dune field model will result in a regular pattern (Section 4.5). Finally, results are summarized and physical implications are discussed (Section 5).

2. Continuum models and dune collisions

The multiscale approach used in this study involves two scales: (i) the continuum dune model is used to observe the behavior of one or a few dunes; (ii) these observed behaviors are then used as the bases of phenomenological rules governing the migration and interaction of particle dunes in the dune field model. Thus, although the main focus of this paper is on results of the large scale (dune field) model, to validate this approach we will first outline the smaller-scale (continuum dune) model and its use in investigating dune collisions.

2.1. Continuum modeling

The seminal work of Sauermann et al. (2001) is the basis for most current continuum models of the formation and evolution of sand dunes. This study constructed a two-dimensional model which considered the evolution of a wind-driven sand flux layer over a dune, and exchanges between this layer and the dune itself. Its main improvement over previous models (Stam, 1996) was the inclusion of a spatial delay (the saturation length) over which the sand flux evolved toward the carrying capacity of the wind. The inclusion of this spatial delay, which had first been observed and measured by Bagnold (1941), fixed the unphysical anchoring/lengthening of the foot of the dune seen in previous models, as well as provided a characteristic length scale related to minimal dune size. Later refinements considered linearized versions of the equations (Kroy et al., 2002; Andreotti et al., 2002b) as well as extension to 3-dimensions (Hersen, 2004).

Although these continuum models have been successfully used in many studies of isolated dune formation (Section 2.2), one drawback to the continuum models is the large number of constitutive equations that must be specified. In developing our own two-dimensional continuum dune model, we have endeavored to identify the ingredients which have a significant quantitative effect on results. With respect to these ingredients (which are outlined below, illustrated in Fig. 1, and given in equation-form in Appendix A), our model deviates little from assumptions used in other continuum dune models:

1. The profile of the near-surface airflow is entirely a function of topography. This profile takes into account airflow separation in regions downwind of sharp changes in slope (sometimes called 'shadow zones'), such as in the lee of the crest of the dune. In these shadow zones, slow air recirculation is not strong enough to transport sand; sand free falls, forming a slip face. The boundary of the shadow zone, the 'separation bubble,' extends downwind from the crest of the dune to the point where it is assumed that aeolian sand transport resumes (Sauermann et al., 2001). While the precise location of flow separation can only be found through fluid dynamic calculations over the detailed dune topography, it is sufficient to phenomenologically approximate this region (Sauermann et al., 2003). We take this route in our continuum model and base our separation bubble shape on studies of airflow over simple dune-like geometries (Schatz and Herrmann, 2005).
2. Using this airflow profile, the shear stress exerted by the wind onto the dune's surface is calculated. The most common approach to computing the shear stress is a linearized approximation for small topography gradients, resulting in a straightforward analytical expression (Jackson and Hunt, 1975). In the shadow zones, the near-surface wind is negligible so the shear stress is generally assumed to be zero.
3. The wind′s shear stress is used to calculate the saturated sand flux, which is the equilibrium amount of sand the wind could move if the wind velocity and topography were homogenous. The actual flux experiences a downwind spatial delay (called the saturation length) in comparison to the saturated flux. This calculation also takes into account the lack of sand deposition or erosion on hard, non-erodible surfaces like bedrock.
4. The dune topography changes via mass conservation with the sand flux.
5. An avalanche-type process forces the dune topography slope to 'instantaneously' adjust to be at or below the angle of repose. In some models (Kroy et al., 2002), this is done by running a separate simulation update after each time-iterative update on the topography, which drops the slope down to or below the angle of repose. In this model, the dune slope is updated concurrently with the mass conservation step by including 'diffusion' of the dune in the mass conservation equation. The diffusion coefficient is set very large when the slope of the dune exceeds the angle of repose, and very small otherwise, with exact values of the diffusion coefficient chosen based on related timescales, to preserve the 'instantaneous' nature of avalanches compared to all other processes.

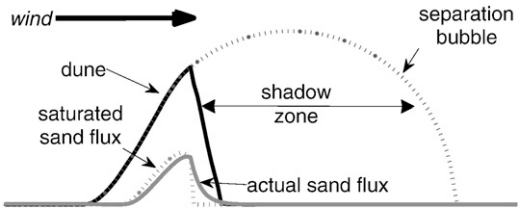

Fig. 1. Schematic diagram showing the variables that are computed in a continuum dune model: dune topography → separation bubble/shadow zone → saturated sand flux (via shear stress calculation) → actual sand flux → dune topography. This diagram is the result of a simulation run, with the vertical scale of each parameter exaggerated for clearer superposition.

2.2. Evolution of isolated dunes

Continuum dune models have been used to quantitively connect dune characteristics to environmental conditions (like sand supply and wind strength) and physical processes (like saltation). For example, studies of isolated dune evolution are able to replicate reasonable dune profiles of many sizes and types (e.g., the two-dimensional profiles shown in Fig. 2, three-dimensional barchan shapes created by (Hersen, 2004)) through consideration of how much sand is available and how the sand is transported. Observed relations, like the inverse relationship between dune height and velocity (Bagnold, 1941), are also replicated and explained.

More recently, the models have been used to study the influences of wind and sand flux on details of dune morphology (Herrmann et al., 2005; Parteli et al., 2006a) and the influence of vegetation and induration in stabilizing dunes (Herrmann et al., 2008). Additionally,

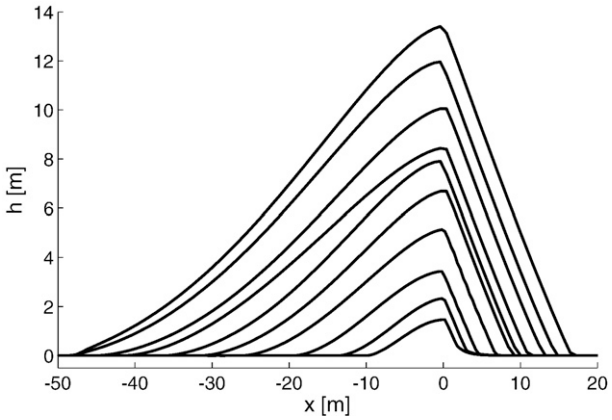

Fig. 2. Sample steady-state two-dimensional terrestrial aeolian dune profiles calculated through numerical simulations. Different dune cross-sectional areas are shown, from a roughly minimal sized transverse dune (dunes with height less than 1 m consist of a convex windward slope with no slipface) to a dune 14 m in height. Note that the vertical axis is exaggerated — the average windward slope for these profiles is 8–16°.

many studies have examined the characteristic scaling of dune formation and evolution in different environments, such as underwater or on Mars (Claudin and Andreotti, 2006; Parteli and Herrmann, 2007).

2.3. Dune interactions

To connect the two scales (dune evolution and dune field evolution), we initialized our continuum dune model with two dunes of specified size, the smaller located upwind of the larger. The initial dune profiles were steady-state profiles calculated during simulations of isolated dune formation. The initial dune spacing was chosen by testing for the minimal distance at which no changes in size occurred immediately in the downwind dune because of the presence of the upwind dune (because of changes in its shear stress and, thus, sand flux calculation). To eliminate a dependence on the sand influx rate (which does appear to influence dune migration and morphology), periodic boundary conditions were used.

In these simulations, the upwind (and smaller, thus faster) dune catches up to the downwind dune. As the shadow zone of the upwind dune impinges upon the foot of the downwind dune, sand in the foot of the downwind dune is not transported by the wind and so is left behind and is eventually absorbed by the upwind dune. As the downwind dune loses sand, its profile gradually becomes shorter, which causes its velocity to increase. Similarly, the upwind dune gains sand, becomes taller, and decreases its velocity. Eventually, the upwind dune begins to climb the downwind dune and the two dunes would lose their distinct shapes and form an amorphous two-humped dune-complex. Sand continues to be exchanged and the humps change in height (the upwind hump grows and the downwind hump shrinks) while moving toward, then (once the downwind hump was the smaller of the two) away from each other (Fig. 3).

Simulations were run with combinations of dunes with cross-sectional areas of 10–400 m^2 (corresponding to initial heights of 1–15 m), and dune pairs were categorized by the resultant type of interaction (Fig. 4).

We noted two qualitatively distinct outcomes: (1) *coalescence* resulted when the downwind hump subsided into the dune complex, resulting in one unified dune, and (2) *ejection* occurred when the downwind hump managed to separate completely, resulting in an exchange of material between the colliding dunes. In a small number of cases, the downwind hump managed to separate but was too small to remain stable and so would eventually *disappear*. We initially examined this case separately, but because it occurred in only a small number of cases, we reclassified it as an extreme case of *ejection*.

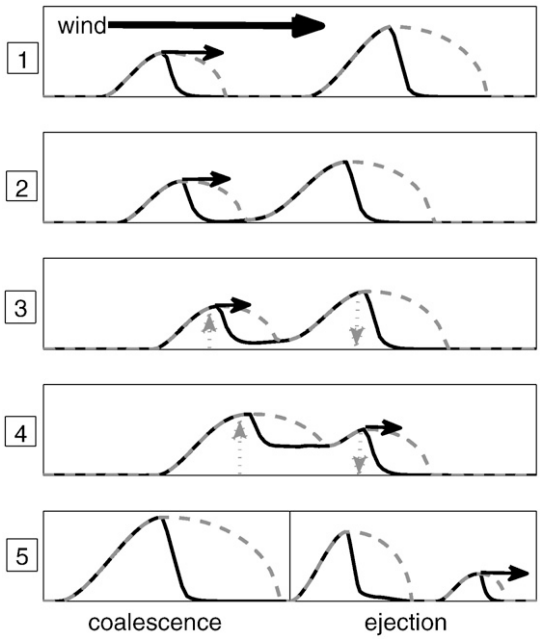

Fig. 3. Schematic diagram illustrating a dune collision. The topography/dune profiles are outlined in black, and the separation bubble is outlined in gray. The horizontal arrows show relative dune motion and the vertical arrows show changes in dune height. From top to bottom: 1. The upwind (smaller) dune approaches the downwind dune. 2. Eventually its separation bubble impinges upon the foot of the downwind dune, arresting that sand. 3. As the upwind dune continues to move toward the downwind dune, it gains sand that the downwind dune leaves behind. 4. As the upwind dune grows and the downwind dune shrinks, their relative crest height reverses, allowing the downwind dune to migrate faster than the upwind dune. 5. If the downwind dune loses all of its sand before it can migrate away, then we have *coalescence*. Otherwise, we have an *ejection* case.

Plotting the different types of dune interactions as a function of the sizes of the colliding dunes (downwind cross-sectional area: A_{before} vs. upwind cross-sectional area: $a_{before}<A_{before}$, Fig. 4), it can be seen that the boundary between coalescence and ejection cases (i.e., the intermediary disappear cases) roughly follows a straight line passing through the origin. Along that line the size ratio between the two dunes before interaction is constant: $r=(a/A)_{before}\approx 1/3$. From this,

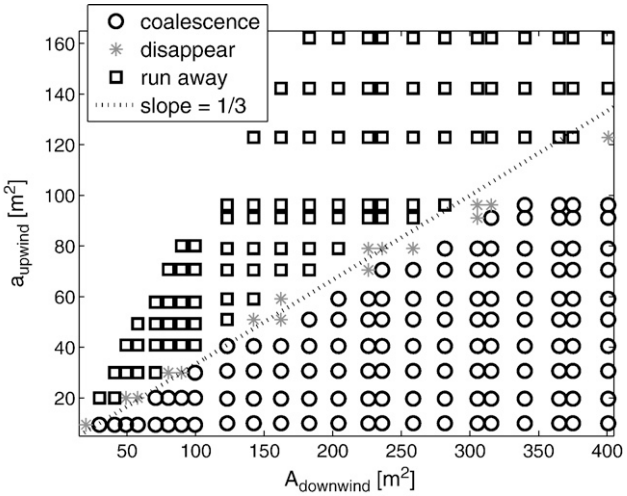

Fig. 4. Plot of the different types of dune interactions as a function of the sizes of the dunes before collision: the area of the downwind dune (A) vs. the area of the upwind/smaller dune (a). Note that the boundary between *coalescence* and *ejection* roughly follows a straight line through the origin with slope of roughly 1/3. This implies that if the dune size ratio before collision: $(a/A)_{before}$ is smaller than 1/3, then coalescence occurs. Conversely, if $(a/A)_{mbefore}>1/3$, then two dunes result.

we can see that if we consider a pair of dunes such that the line from that point (A,a) to the origin is less steep than that boundary (equivalently, the size ratio of the two dunes is between 0 and 1/3), coalescence occurs. Conversely, when the line between a point and the origin is steeper than the boundary (or the size ratio is between 1/3 and 1), the collision results in two dunes or ejection. Thus, it is appears that the size ratio (r) between the dunes is what determines a collision result, not the individual sizes of the dunes.

To understand in more detail what will result when two dunes collide, we also compute the size ratio of the dunes after collision ($f(r) = (a_{downwind}/A_{upwind})_{after}$; where $a_{downwind,\ after} = 0$ if the dunes coalesce), and plotted this against the size ratio before dune collision (r). Resultant dunes which disappear are treated as very small ejection dunes because the sizes are measured as soon as the dune-complex separates into two dunes. As can be seen in Fig. 5, the data falls roughly on a single curve and indicates that the relevant quantities are the ratios of dune sizes before and after collision. We call this relationship the *interaction function* $f(r)$. When the ratio r is smaller than about 1/3, $f = 0$ indicating coalescence. In the limit where very similarly sized dunes collide, $f(r)$ increases and appears to $\rightarrow 1$.

Similar results have been found elsewhere in the literature. For example, studies of discrete numerical simulations of interacting three-dimensional barchan dunes (Katsuki et al., 2005) and laboratory experiments of subaqueous barchan dune collisions (Endo et al., 2004) yield results which support our hypothesized interaction function characteristics. Additionally, a study by Durán et al. (2005) using continuum numerical simulations of three-dimensional barchan dune interactions found an interaction function (Fig. 6) which also consists of a continuous relation between size ratios before and after collision, with $f(0) = 0$ and $f(\rightarrow 1) \rightarrow 1$.

2.4. Dependencies of the interaction function

As explained in Section 2.3, the balance between the timescale over which the upwind dune merges with the downwind dune and the rate at which the downwind dune shrinks (and migrates faster) is what determines the end result of a collision.

For example, the timescale over which the dunes merge is very short if dunes initially have very different sizes, as the relative velocity between the dunes is large. The dunes will merge together before the downwind dune can shrink sufficiently to escape, which is why $f(0) = 0$.

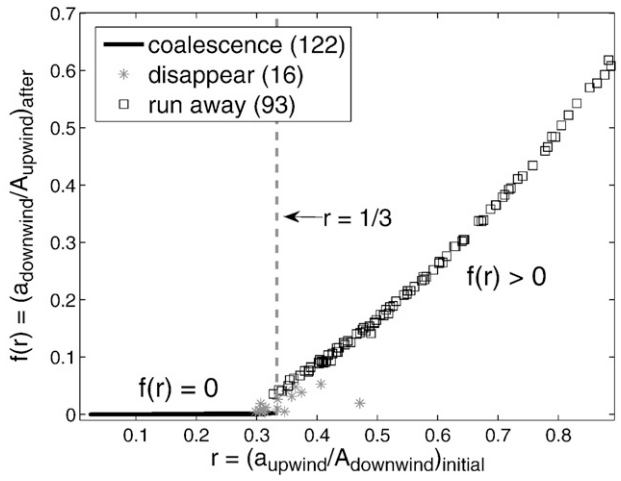

Fig. 5. Plot of the area ratio of colliding dunes, before collision vs. after. Note the distinct zones of interaction results: coalescence occurs when the dune size ratio before interaction is below some threshold (1/3); when the ratio is above that threshold, then the output size ratio generally falls along a specific curve, independent of the absolute sizes of the dunes (the outlier corresponds to the smallest dune pair sampled). In the legend, the numbers given are the total number of simulations which yielded that particular type of interaction.

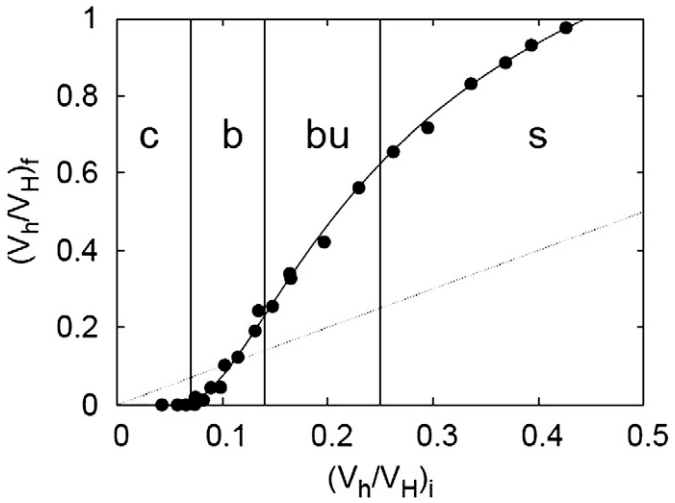

Fig. 6. This plot was derived for three-dimensional barchan dune collisions by Durán et al. (2005) and shows volume ratios of colliding barchan dunes before vs. after collision (the dots, along with a best fit curve). It exhibits the same characteristics as the interaction function shown in Fig. 5: a threshold between coalescence (c) vs. all ejection-type interactions (b/bu/s; breeding, budding, solitary waves), a single monotonic curve along which all points fall and which passes through (0,0) and probably (1,1). The straight line shown has a slope of one.

Conversely, the rate at which the downwind dune shrinks is more important if dunes are initially very similar in size, because the relative velocity will be low. As they will move towards each other over a long time period, the downwind dune will be able to slowly escape after becoming slightly smaller than the upwind dune. The two dunes will end up close to each other in size, so $f(r) \rightarrow 1$ as $r \rightarrow 1$.

A continuum between these two effects is expected, as the timescale over which dunes interact will increase as the disparity between the sizes of the two dunes increases. This yields a continuous, monotonic function. The exact form of the function will depend on factors which set the timescale over which the dunes interact and the rate of the sand exchange between the dunes.

In the continuum dune model, for example, one way to change the rate at which sand is exchanged is by increasing the aspect ratio of the separation bubble. This lengthens the shadow zone of the upwind dune, causing the foot of the downwind dune to be caught in that shadow zone and arrested sooner. The downwind dune, thus, loses more sand before the upwind dune begins to gain sand. As the growth of the upwind dune is delayed relative to the shrinkage of the downwind dune, the downwind dune will need to shrink more to become the smaller of the two. When the downwind dune is finally ejected, it will be smaller (and the upwind dune will be larger), causing the interaction function to be lower (i.e., $f(r)$ will decrease over all values of r where $f(r) > 0$). Conversely, if the length of the separation bubble is decreased, then the interaction function will be higher. Test simulations have shown this to be the case, although the effect was small (Fig. 7).

2.5. Implications of the interaction function and crossover value

Our derivation of an interaction function for transverse dunes (Fig. 5) is included in this study to explain the general form of an interaction function. The specific function that was found through our two-dimensional dune simulations, however, will not be used in the remainder of this study because that functional form (where for all r, $f(r) < r$) yields coalescence-dominated dynamics.

When $f(r) < r$ for all values of r, then in every collision the larger dune grows and the smaller dune shrinks. As the smaller dune in every collision shrinks and eventually coalesces with the larger dunes (for small enough r, $f(r) = 0$), the dune field perpetually evolves into a

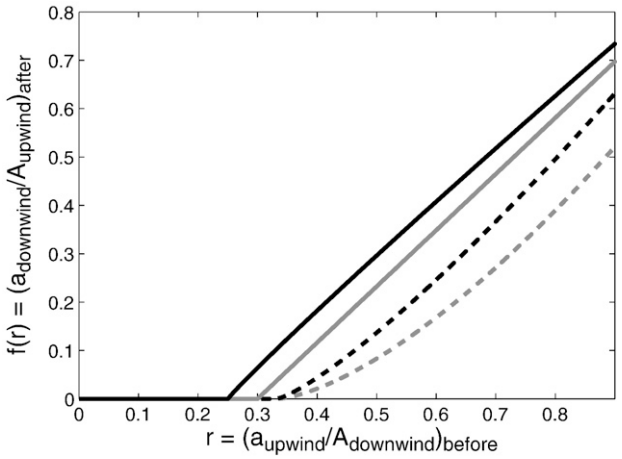

Fig. 7. This plot shows the best-fit interaction functions for transverse dunes, after using different separation bubble aspect ratios in the continuum dune model (e.g., aspect ratio = 6 corresponds to the data shown in Fig. 5). As hypothesized, an inverse relationship between $f(r)$ and the separation bubble aspect ratio exists because of the influence of the ratio on how quickly the downwind dune is able to lose sand.

system containing a smaller number of larger dunes. It should be apparent that this type of dune field dynamics will never yield a stable pattern of similarly sized dunes.

Conversely, when $f(r)>r$ for all values of r, then in all collisions the dunes become more similar in size. Eventually, after many collisions, the dune field will always evolve into a system of many similarly sized dunes (with any remaining collisions occurring around $r\sim1$).

As one more extreme example: if $f(r)=r$ for all values of r, then dunes will behave similar to solitons in that all interactions will preserve the sizes of the dunes involved, as if the dunes simply pass through each other.

Most natural dune field interaction functions will not correspond with one of these examples (in particular, see Livingstone et al. (2005) for a discussion about the unphysical nature of the soliton example). Instead, a natural dune field interaction function will probably be a combination of these extreme examples, with some regions where $f(r)<r$, some regions where $f(r)>r$, and transition points where $f(r)=r$. In these cases, the dynamics of the dune field can be determined based on the interaction function *crossover value*: the value r_* such that for all higher $r<1$, $f(r)>r$. We define the crossover value as the lower bound on the region *connecting to (1,1)* where $f(r)>r$. An interaction function may have several regions where $f(r)\geq r$, but only the region including (1,1) is of interest, as it is necessary for $f(r)>r$ as $r\rightarrow1$ for interactions to actually push the system toward a field where all dunes are about the same size. Additional lower regions where $f(r)>r$ will affect the timescale over which the system evolves, but not the end state.

For the first and third extreme examples discussed above ($f(r)<r$ and $f(r)=r$), $r_*=1$ and the system will never have a stable patterned structure. In the second example considered ($f(r)>r$), $r_*=0$ and the system will always achieve a pattern of similarly sized dunes. The interaction function derived for barchan dunes is an example of an intermediary case ($r_*\sim0.12$ in Fig. 6), so this interaction function *may* yield a patterned structure, and it did in Durán et al. (2005).

Thus, for a dune field model to possibly form a stable patterned system, its interaction function needs to have $r_*<1$. Generic interaction functions with this characteristic (in addition to those characteristics outlined in Section 2.3) will be considered in constructing the dune field model.

3. Multiscale dune field models

As in other works (Lima et al., 2002; Parteli and Herrmann, 2003; Lee et al., 2005), we utilize a multiscale approach by using the continuum model to understand interaction of a small number of dunes. Specifically, the interaction function is based upon the observed dynamics of colliding dunes in the continuum dune model. The dunes themselves are treated as particles with morphologies and dynamics approximated using simple phenomenological relations — without consideration of the detailed results of the continuum model.

The focus of this study is on whether a dune field will form a stable, patterned structure, so simulations are run until it is apparent that field dynamics have stabilized in one of the end states (defined in Section 4.1).

3.1. Approximation of single dunes

Rather than keep track of every degree of freedom in the continuum model, it is useful to only track dunes according to their size and location. To determine when dunes are close enough to interact, we make reasonable assumptions about their morphology. Their shape is assumed scale-invariant, approximated as triangular wedges, with a stoss aspect ratio of 10 (Parteli et al., 2006b), a lee aspect ratio of 1.5 (the angle of repose), and a separation bubble with an aspect ratio of 6 (Schatz and Herrmann, 2005), as shown in Fig. 8.

The dunes move with a velocity inverse to their crest height (Andreotti et al., 2002a); i.e., $v\sim k/H$. The coefficient k varies between actual dune fields (Bagnold, 1941). In this study, it is arbitrarily set at 100 m^2/yr.

3.2. Interactions and initialization

Collisions occur when the foot of the downwind dune is touched by the separation bubble of the upwind dune. The distance between dunes after collision is calculated the same way, with the downwind dune located just outside the separation bubble of the upwind dune.

The results of dune collisions are governed by the interaction function, which relates the size ratio of the dunes before collision to the size ratio of the dunes after collision (as described and derived in Sections 2.3–2.5). In our dune field model, collisions occur instantaneously once dunes are close enough to interact.

Initial cross-sectional areas for the dunes (for either initial or influx dunes) are taken from a specified range with uniform distribution. When we consider a semi-infinite domain with an upwind influx of dunes, we assume a constant mass influx rate of 30 m^2/yr to relate injection frequency to dune size. In general, this corresponded to ~1000 influx dunes per 1000 years for simulations run with a small mean dune size ($M=40$ m^2), and ~400 when a larger mean dune size ($M=100$ m^2) was used.

3.3. Model assumptions

As the entire point of our study is to examine which model assumptions influence simulation results, we will highlight and explain several assumptions we have made (in decreasing importance):

1. *Sand flux effects are ignored.* This means that dunes only change size when they collide and the total size of colliding dunes is conserved during a collision (i.e., $(a+A)_{before}=(a+A)_{after}$). In reality, sand can

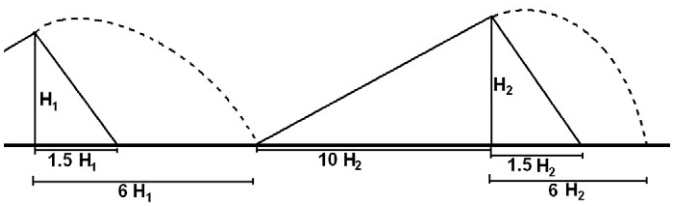

Fig. 8. Approximation of the morphology of a dune, with fixed stoss aspect ratio of 10 and lee aspect ratio of 1.5. This shape is used to determine the dune's zone of influence as a function of area — two dunes interact when the separation bubble (with aspect ratio of 6) of the upwind dune touches the foot of the downwind dune, as shown.

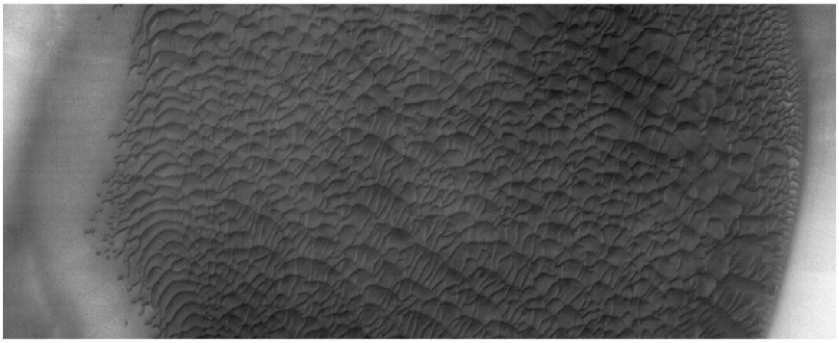

Fig. 9. This image (HiRISE PSP_008628_2515; image's small side has 6 km length) shows a Martian dune field within a crater. Except for near the boundaries of the field (where topography is probably influencing dune evolution), all dunes appear to be one of two sizes, as if two patterns are superimposed. Such pattern superposition can occur through multiple generations of dune construction and evolution, where in each generation the dune field tends towards a simple pattern through dune interaction (Kocurek and Ewing, 2005).

be lost or gained by dunes between and during collisions (Elbelrhiti et al., 2008). Including this sand flux, however, adds an additional layer of complexity on the model, and such processes are not currently constrained by observations or experiments. The effect this assumption may have on simulation results will be addressed in Section 5.1.

2. *The interaction function is assumed to be spatially and temporally constant.* Dune collisions occurring at different times or locations are assumed to obey the same interaction function. The interaction function, however, may depend on local conditions, such as the type of sand included in the dunes. As timescale is not considered, in this study it is not important that the interaction function may change shape. If the interaction function crossover value should change temporally or spatially, however, as is suggested in Besler (2002), then this could impact the end state of the dune field. The physical implications of this will be discussed in Section 5.1.
3. *Collisions happen instantaneously.* We considered this to be an acceptable approximation as we observed that the time between collisions was much longer than the collision timescale in our simulations. Additionally, this simplifies the collision-dynamics as generally only two dunes can collide at a time.
4. *Dune sizes are chosen from a uniform distribution.* Although physical systems generally have other types of distributions (e.g., Gaussian), a uniform dune size distribution will be used in this study as its structure is the simplest. This will remove one level of complexity from analysis of simulation results. Additionally, we will discuss the effect of a Gaussian distribution of dune sizes in Section 5.1.
5. *The dune shape and zone of influence are specified somewhat arbitrarily.* Both of these will affect the timescale of dune field evolution, and the zone of influence directly relates to the interdune spacing of a patterned system. These values will have no effect, however, on whether or not a system will form stable similarly-sized dunes, which is the focus of this study.
6. *The value of the constant influx rate and the coefficient in the velocity relation are also arbitrarily specified.* Again, both of these constants will play a role in the timescale over which the field attains its end state. As long as dunes are not injected on top of one another, they have no other influence on the simulation.

4. Model results and the influence of structural elements

The purpose of this study is to examine whether various structural elements in dune field models influence the overall evolution in our model, and specifically how the different elements will change the end state of a simulation. We do this by varying the interaction function, boundary type, and initial/influx conditions.

4.1. Simulation end states

This portion of the study is concerned with the long-time behavior of dune fields, rather than individual dunes. In this study, we show that a dune field can evolve towards two possible outcomes. In one scenario, a dynamic equilibrium is established where all dunes are and remain similar in size; we call this end state *quasi-steady* (for example, the crescentic dunes in White Sands, New Mexico or the Martian dune field shown in Fig. 9). The other possibility is *runaway growth*, with one or a few dunes continually growing through coalescence with upwind dunes (a possible example of this type of dune field structure on Mars is shown in Fig. 10).

Let us emphasize that because we are concerned with only the end state of a simulation, the exact timescales for evolution are not considered in the following tests. The effect timescale will have when model results are compared with actual dune fields will be discussed in Section 5.1.

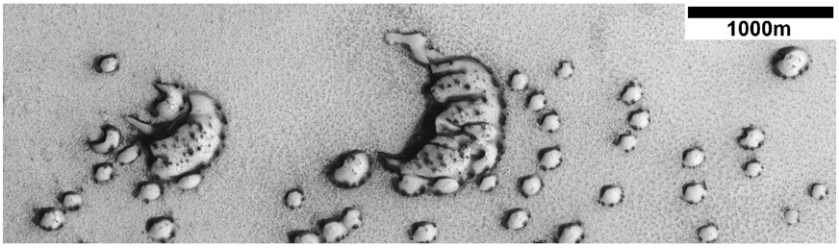

Fig. 10. This image (HiRISE PSP_007172_2570) shows a Martian dune field where runaway growth appears to be occurring. Many small, uniform barchan dunes (~200 m wide) populate this area, interspersed with a small number of large megabarchans (large, central one is ~104 m wide). All dunes have left-facing slipfaces, implying that they formed under the same environmental conditions and were (are?) migrating towards the left. The megabarchans have sinuous crests and multiple slipfaces on the windward slope, implying that these dunes formed through collision of the barchans (a hypothesis also put forward by Bourke and Balme (2008)). The areas downwind of the two megabarchans shown are mostly devoid of other dune structures, implying that the collisions are predominantly resulting in coalescence. There are no apparent topographical or environmental reasons for the size disparity between the megabarchans and the barchan dunes.

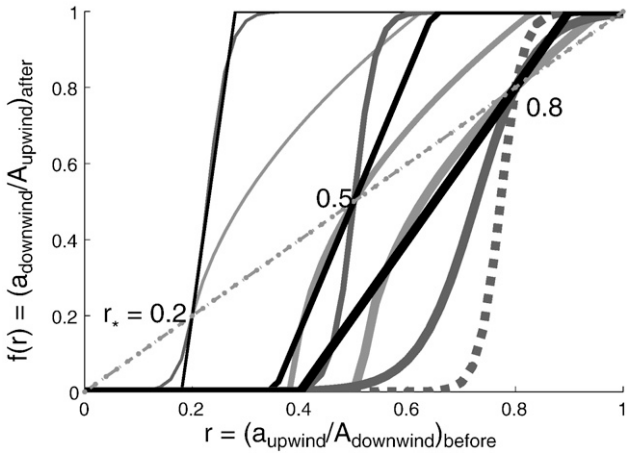

Fig. 11. The interaction functions used to study the influence of the interaction function forms: linear (black), tanh (dark gray), and square root (light gray). The dash–dotted line is included to highlight the functions' crossover (r_*) values. For the functions with $r_*=0.2$ (thin) and 0.5 (medium thickness), the coalescence zones were chosen to have similar extents. For the functions with the $r_*=0.8$ (thick), three had the same coalescence zone and one had a much longer coalescence zone (dashed).

In the *quasi-steady* end state, all dunes have approximately the same size and interdune spacing — the epitome of a patterned dune field. Since the dunes are similar in size, they will move with approximately the same velocity and, thus, rarely interact with each other. The interdune spacing will also be similar across the field, as this quantity depends on their defined zone of influence, which depends on their size (Section 3.2). Even if new dunes are introduced (e.g., through an influx condition), interactions ultimately yield dunes of similar size with the rest of the field. This end state is characterized by a constant number of dunes (close to the initial number) when no influx occurs, or a linear increase in the case of influx. This implies a steady mean dune size and mean interdune spacing (e.g., Fig. 14a).

In the runaway growth case, one or a few dunes become large enough relative to their surrounding dunes that all future interactions occur between very disparately sized dunes (r small), which results in the larger dune getting still larger (and coalescing with all smaller upwind dunes). In this case, the system eventually settles into a size-sorted field, with dune size monotonically decreasing with distance from the upwind boundary, and with a near-constant number of dunes (but significantly less than the total initial number) even when an influx occurs. In the case of periodic boundaries (meant to simulate an infinite environment), the final outcome is just a single large dune after a period in which the mean dune size and interdune spacing continuously grow (e.g., Fig. 14c).

4.2. Influence of the interaction function

As described in Section 2.4, the interaction function is based on the collision-dynamics of a dune field, which will depend on local environmental conditions such as wind speed and sand supply, as well as on the detailed physics of aeolian sand transport and airflow over complicated dune geometries. Experiments and observations have not yet yielded information about constraints of interaction functions for a particular dune type or field. Numerical simulation of dune collisions can provide an interaction function (Section 2.3), but even this approach has not yet been validated.

With this in mind, we will constrain possible interaction functions $f(r)$ only with those characteristics that were explored in depth in Sections 2.4, 2.5: (i) a continuous, monotonic function with $f(0)=0, f(1)=1$, (ii) that has a coalescence threshold ($f(r)=0$ for small r), (iii) and a crossover value $r_*<1$ ($f(r)>r$ for $r_*<r<1$).

By running simulations with several generic interaction functions, we aim to discover which characteristics of the interaction function (e.g., coalescence threshold, function steepness, crossover value) influence the simulation's end state. For example, as discussed in Section 2.5, it is hypothesized that an interaction function crossover value will affect the end state of the simulation.

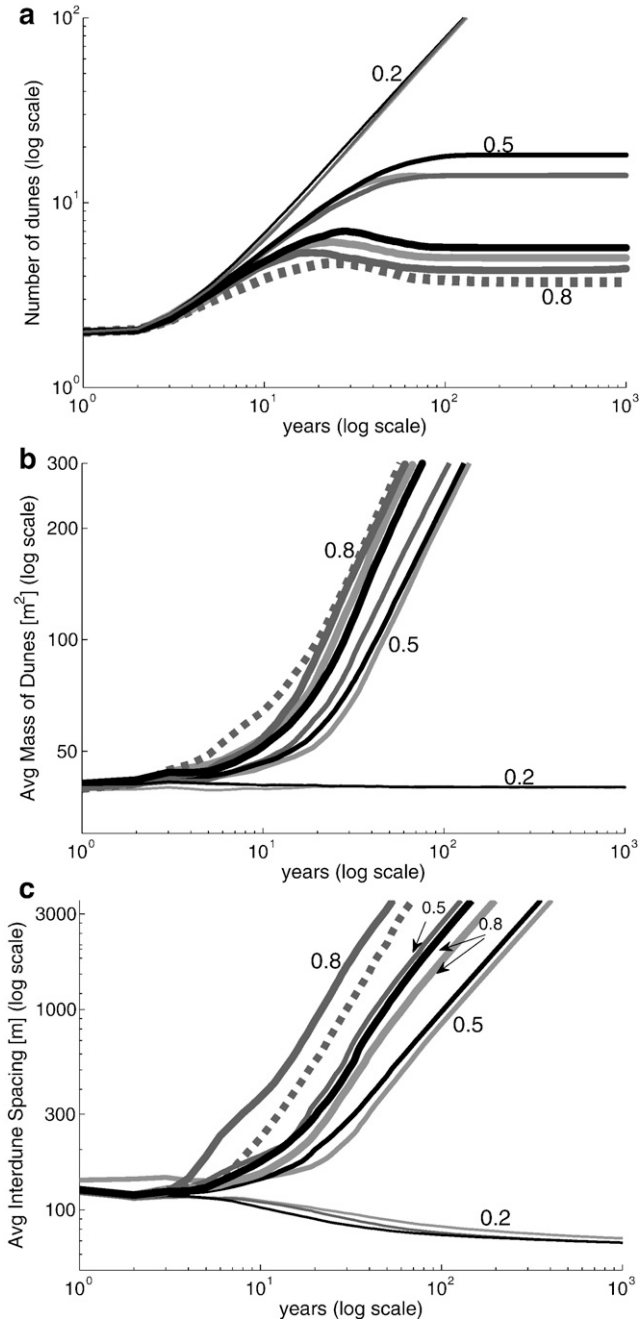

Fig. 12. Plots showing the averaged results from 250 dune field simulation runs with each different interaction function (line styles match those used in Fig. 11). All simulations were run with semi-infinite boundary conditions. From the top, the following system observables are plotted as functions of time (log–log scale): the number of dunes in the system, the average dune size, and the average interdune distance. When the crossover value is 0.8 (thick) or 0.5 (medium thickness), then runaway growth occurs: the number of dunes is limited and the average dune size/spacing grow in time. Quasi-steady state behavior occurs when the crossover value is 0.2 (thin): the number of dunes increases linearly and the average dune size/spacing approaches a constant. Although not included in these plots, the standard deviation for each set of runs was also the same for all functional forms with the same crossover value.

Identifying influential characteristics of interaction functions will allow us to classify the infinite number of possible interaction functions according to a finite number of important characteristics. This will greatly simplify the rest of this study, as a few test interaction functions will adequately represent all possible interaction functions. Additionally, this will simplify future attempts to place constraints on a dune field's interaction function based on observations and/or laboratory experiments.

We considered the following interaction functions:

1. $f(r) = \tanh((r-k_1)k_2\pi)/2 + 1/2$: this functional form provides a smoothed step function from $0 \rightarrow 1$, with adjustable steepness;
2. $f(r) = k_3(r-k_4)$: the simplest functional form;
3. $f(r) = k_5\sqrt{r-k_6}$: this functional form is loosely based on the function used in Lee et al. (2005) to model transverse dune fields;

where in all cases we define $f(r) = 0$ if the range is negative, and $f(r) = 1$ if the range is >1. The k_i values are left as free parameters so that the crossover value as well as the extent of the coalescence zone can be specified. Examples are shown in Fig. 11.

In the tests, a semi-infinite boundary was used with an influx of dunes with area chosen from a uniform distribution of 10–70 m^2. We averaged the results of 250 simulation runs with each test function to eliminate any dependence on the randomly chosen influx dunes.

Fig. 12 shows simulation evolution when using different interaction functions. The steepness and coalescence threshold of the function do not appear to have any significant effect on the end state of the simulation. These functional characteristics also did not significantly influence the average area of the dunes (Fig. 12). In contrast, the average interdune spacing, which was hypothesized to depend on the functional form as it would depend on the rate at which dunes changed size when runaway growth occurs, did vary significantly between functional forms when $r_* = 0.5$ or 0.8.

This shows that the precise details of the interaction function are unimportant — only the interaction function crossover value has a significant influence on the end state of the simulation. Based on this, we adopt simple linear functions (Fig. 13) for the remainder of this study, where the only adjustable parameter is r_*.

4.3. Influence of boundary types

Periodic boundary conditions are often used in the design of numerical simulations because they simplify the structure of the simulation. With periodic boundary conditions, outflux from the simulation box equals influx and the simulation box remains the same size throughout the simulation run. When modeling the evolution of a dune field, this corresponds to simulating the evolution within a subset of the dune field and assuming the entire dune field is roughly approximated by infinitely tiling that subset to fill the field. This only makes sense if one is considering the evolution of a portion of a dune field sufficiently far away from any boundary effects (e.g., dune initialization or topography), and the dune field is assumed to be sufficiently regular that just a section of it can be considered representative of the entirety.

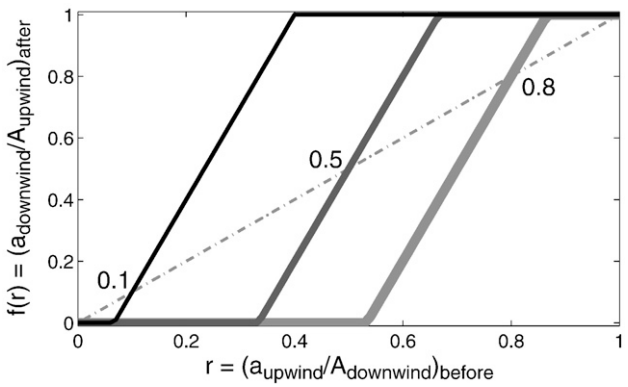

Fig. 13. Examples of the simple, linear interaction functions ($k_3 = 3$, $k_4 = 2r_*/3$) used in the remainder of this study; $r_* = 0.1$ (thin), $r_* = 0.5$ (medium), and $r_* = 0.8$ (thick). As was shown through tests, the exact functional form is not important when considering the end state of the simulation — only the crossover value (r_*) matters. Thus, linear functions like these can be used as valid representatives of all reasonable interaction functions with the same r_*.

For many interesting problems associated with dune fields, however, boundary effects cannot be ignored. Additionally, if the dunes are assumed to vary across the simulation box, then one needs to justify the assumption that the dunes that leave the simulation box are equal in size and spacing to the dunes that enter. The size of the simulation box and the initial number of dunes also set (potentially unphysical) limits on dune number, size, and spacing.

In the cases where a dune field is thought to differ spatially and/or boundary effects (such as dune formation) are of interest, semi-infinite boundaries are more physically realistic. In this case, as the name implies, one boundary is fixed (i.e., the influx condition is specified) and the other is open, allowing the simulation box to lengthen as dunes migrate. Although more physically intuitive when considering the evolution of an entire dune field and including the effect of its source region (as was done in Lima et al. (2002)), the influx boundary condition unfortunately requires constitutive specifications such as statistics of new dune size and frequency.

One can, of course, use semi-infinite boundary conditions with no influx (or a temporary influx, as was used in Lee et al. (2005). This allows the simulation box and interdune spacing to expand indefinitely and allows for variations in field structure, without great concern over how the influx is defined. Because two dunes will not collide with each other unless the smaller dune is upwind, however, field evolution will be arrested once it becomes size-sorted. Additionally, because no new dunes are introduced past a certain time, this sets a limit on the number and sizes of dunes in the field, which does need to be justified.

We investigate the effect of using these three different boundary conditions:

1. semi-infinite boundary conditions with an influx and no initial dunes. The sizes (measured by cross sectional area) of input dunes were chosen randomly from a uniform distribution of 10–70 m^2;
2. semi-infinite boundary conditions with no influx and an initial number of dunes equal to the total number of influx dunes in case (i) at time 1000 years. These initial dunes were randomly spaced, with an average spacing of 50 m, and initial sizes were also taken from 10–70 m^2;
3. periodic boundary conditions with the same initialization of dunes as case (ii). The simulation domain had a length of 50 m times the number of dunes.

With each boundary condition, 250 simulations were averaged together for each crossover value: 0.1, .2, .3,…, .9.

In simulations run with low crossover values ($r_* \leq 0.3$), all boundary conditions yielded a quasi-steady end state; i.e., all dunes became and remained similar in size (Fig. 14a). In the cases with no influx (semi-infinite and periodic) the total number of dunes was conserved. Of course, in those two cases, the spacing between dunes differed because of the constant length of the periodic boundaries' simulation box. With semi-infinite boundaries and influx, the number of dunes in the system increased linearly with time.

When simulations were run with high crossover values ($r_* \geq 0.5$), similar low numbers of dunes were achieved by all simulations (Fig. 14c). Again, however, the total mass of the system (and the maximal dune size) was limited for the two cases without influx. This also changes spacing relations, since dune velocity is related to dune size.

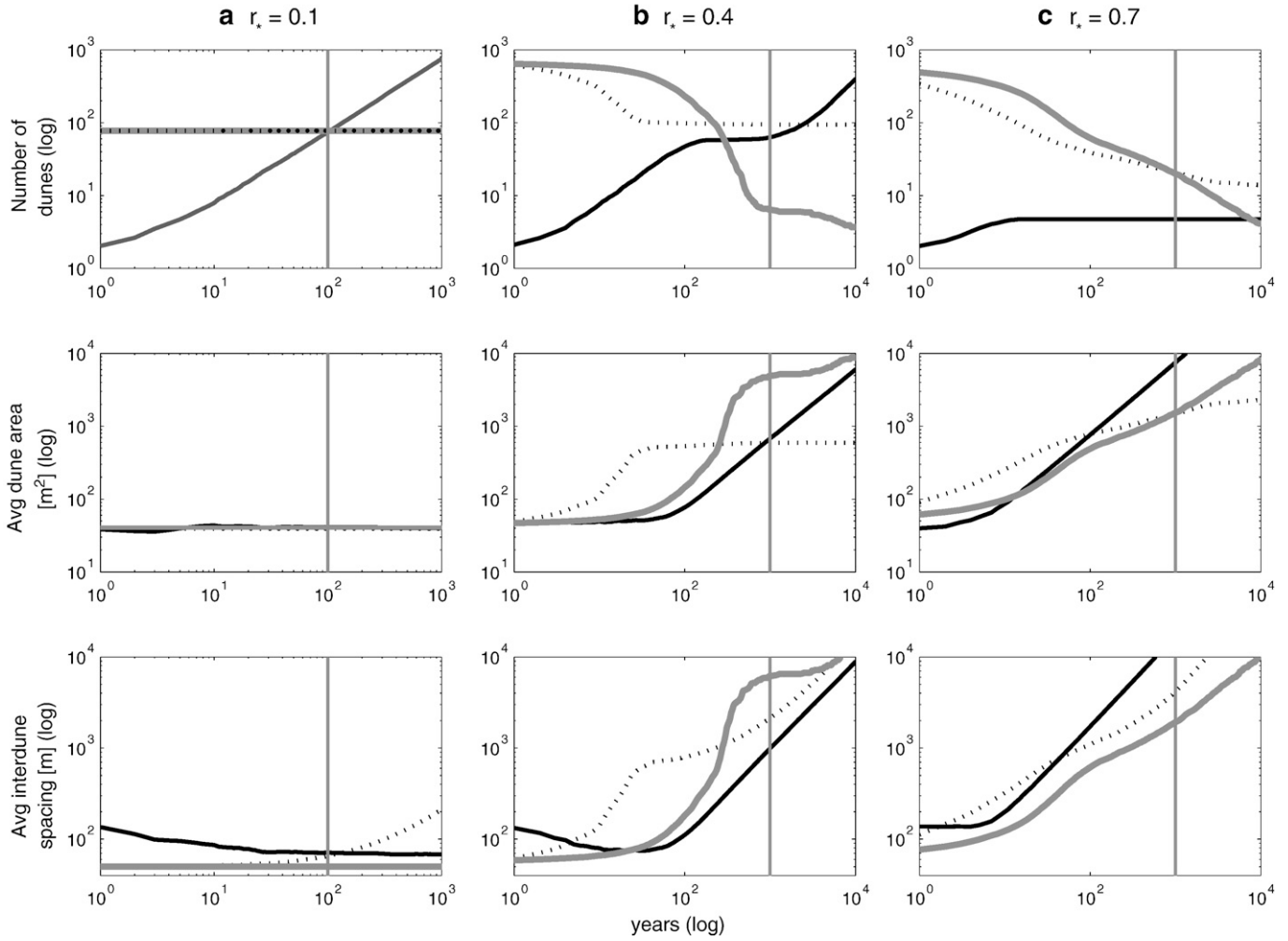

Fig. 14. Plots showing the dynamic behavior of simulations run with different boundary conditions: semi-infinite boundaries with an influx and zero initial dunes (black solid), semi-infinite boundaries with initial dunes and zero influx (black dotted), and periodic boundaries with initial dunes (gray solid). In the two cases with initial conditions, the number of initial dunes was equal to the total amount of dunes put into the influx of the third case, at the time indicated with the vertical gray line. If different boundary condition cases created similar systems, then we would expect the cases to show similar trends at and around that time. From the top, the following system observables are plotted as functions of time (log–log scale; averaged values over at least 250 runs): the number of dunes in the system, the average area of the dunes, and the average distance between dunes. As we can see, having a nonzero influx and/or initial condition greatly affects the dynamics, but the end state of the simulation.

The largest differences were observed for the intermediate crossover value (0.4). As can be seen in Fig. 14b, the system exhibits different dynamics between the cases. Of course, large differences were also seen between runs with the same boundary conditions (as this value apparently is near the boundary between the two end states), making it difficult to interpret the results of the simulation in a meaningful manner.

With all boundary conditions, the end state of the simulations obviously and consistently depended on crossover value. Measurements of dune sizes and spacings differ between the cases, however, making it difficult to accept more detailed interpretations based on simulations run with unjustified boundary conditions.

In this study, we are interested in the evolution of the entirety of the dune field (including the effect of dune initialization) towards an end state. Thus, in the remainder of this paper, we will focus only on semi-infinite boundary conditions with continuous influx.

4.4. Influence of initial and influx conditions

If dune fields self-organize, an important question is whether the resulting pattern is related to local environmental conditions that drive dune formation (e.g., the initial dune sizes and spacings that may result from topographical or wind variations), or the physics and environmental parameters which affect dune collisions. It is, therefore, important to evaluate whether the modeled system retains memory of how dunes are initialized.

Dune initialization can be included in dune field models via:

1. *an initial condition:* dunes are scattered throughout the field at the start of the simulation run. This corresponds to a 'temporal' beginning to the dune field — dunes have formed and are dispersed throughout a field. At some time (the start of the simulation), collisions between dunes become the only evolutionary process.
2. *an influx condition:* dunes are injected into the simulation box at one boundary. This relates to a 'spatial' beginning to the dune field — dunes form and evolve just outside of the closed boundary of the dune field (resulting in some influx size distribution and rate). Once these dunes enter the field, then collisions become their only evolution process.
3. a combination of these two conditions.

To study the influence that the (temporal and spatial) initial dune sizes have on simulation results, we ran simulations with semi-infinite boundary conditions and constant influx rate. Initial dune sizes were chosen from uniformly distributed size populations with a 'small' ($M = 40$ m^2; e.g., 10–70 m^2) or 'large' ($M = 100$ m^2; e.g., 80–120 m^2)

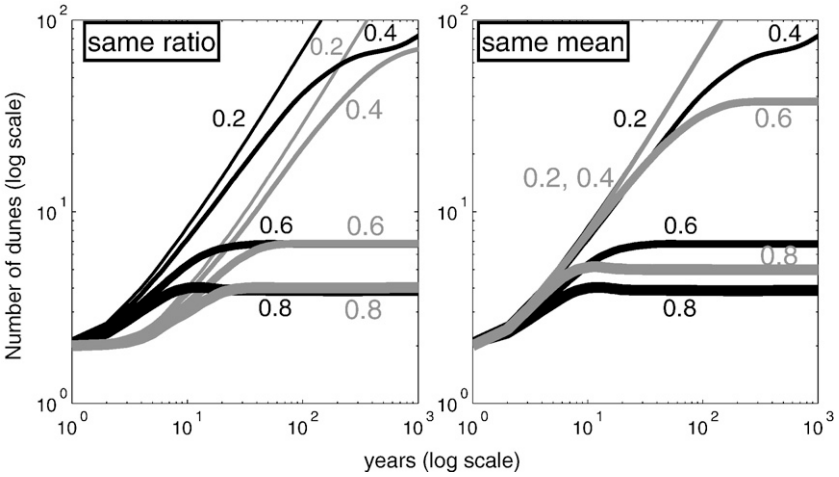

Fig. 15. Evolution of number of dunes (vs. time, both on logarithmic scales) in simulations with $r_* = 0.2$, 0.4, 0.6, and 0.8 (larger crossover value corresponds to an increased line thickness), and with influx dune ranges of 10–70 m^2 (black, both), 25–175 m^2 (gray, left), and 25–55 m^2 (gray, right). This illustrates the influence of having the same mean (right) vs. having similar ratios between the standard deviation and the mean (left). In the plot where the ratio is the same ($\sigma/M \sim 0.43$; $M = 40$ (black) and $M = 100$ (gray)), the end states achieved are similar for the same crossover values. In the plot where the standard deviation is different while the mean is the same ($M = 40$ m^2; $\sigma/M \sim 0.43$ (black) and $\sigma/M \sim 0.22$ (gray)), the end states achieved differ for the same crossover values.

mean dune cross-sectional area, and different standard deviations (e.g., $\sigma \sim 17.3$ for 10–70 m^2 and $\sigma \sim 8.7$ for 25–55 m^2).

The effect of including initial conditions was first examined by running simulations of dune fields with an influx and 0, 10, or 100 initial dunes (with initial dunes chosen from a similar distribution as the influx dunes). Simulations showed that as long as the initial dunes are similar in size to the influx dunes, the initial dunes eventually become indistinguishable in size and spacing from the colliding influx dunes. For example, when the system moves toward a quasi-steady state the mean dune size is the same regardless of the number of initial dunes. If the initial dunes are much larger than the influx dunes, however, then the system is pushed toward runaway growth. Alternatively, if the initial dunes are much smaller than the influx dunes, then the majority of the initial dunes simply run out in front of the dune field that results from the influx.

Thus, we see that the memory of initial conditions is not retained unless the initial dunes are significantly larger than the influx dunes. Because there is no reason to generally assume that initial dunes should be larger than influx dunes, in the remainder of the study we will neglect initial conditions.

In testing for the effect the influx distribution will have on simulation results, we again average 250 simulations together for every interaction rule crossover value, influx mean, and influx standard deviation.

In Fig. 15, we see that the end state of a simulation depends on the standard deviation/mean ratio of the influx dune size distribution (σ/M). For example, the lowest crossover value that results in runaway growth is $r_* \sim 0.4$ for the dune ranges of 10–70 m^2 and 25–175 m^2 ($\sigma/M \sim 0.43$); the lowest crossover value resulting in runaway growth for an influx dune range of 25–55 m^2 is $r_* = 0.6$ ($\sigma/M \sim 0.22$).

4.5. Threshold between end states

Our results show that a dune field's end state depends only on the interaction function crossover value and influx dune size distribution's standard deviation/mean ratio. The way in which these two parameters are coupled can be seen most clearly in Fig. 16, which shows a simulation's end state as a function of r_* and σ/M. A boundary between parameter values yielding a quasi-steady or runaway growth end state clearly exists. To understand this coupling, we utilize a probabilistic approach to predict the evolution of a dune field.

As it is not clear how to estimate the probability that a dune field will enter a specific end state, we instead ask how probable it is that a single collision involving an individual downwind dune of mean influx size (M) will involve an upwind influx dune of size a such that $r = a/M > r_*$, or $a > Mr_*$? As discussed in Section 2.5, interactions involving $r > r_*$ push the dune field towards a quasi-steady end state because the collision results in more similarly-sized dunes.

The reason that the probabilistic outcome of an individual dune collision should be related to the predictions of a dune field's end state results from the nature of the runaway growth end state: the runaway growth end state involves a small number of dunes becoming substantially larger than the rest of the dune field through collisions. If the probability is low that interactions between subsequent influx dunes (i.e., near the beginning of the dune field) will yield dunes more similar in size ($r > r_*$), then it is more likely that a single dune can eventually become disparately large enough to enter into runaway growth. Furthermore, as runaway growth involves a dune growing through collisions, the initial size that we consider is somewhat arbitrary — so we consider the probability with regards to the mean sized influx dune.

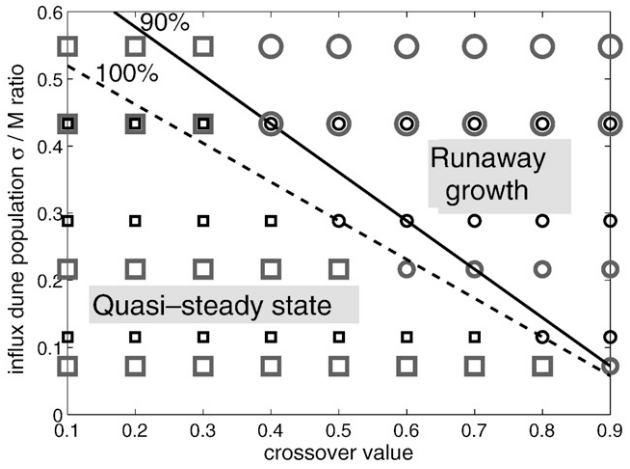

Fig. 16. Plot showing the model end state, as a function of the interaction function crossover value and the standard deviation/mean ratio (uniform distribution). Notice the clear boundary between the regions corresponding to each end state: quasi-steady state (squares) vs. runaway growth (circles). This boundary is consistent between simulations with a mean influx dune size of 40 m^2 (small point markers) and 100 m^2 (large point markers). Additionally, it is not linear, but is roughly bounded (when standard deviation < 0.5 mean) by the trendlines corresponding to a 100% (dashed) and 90% (solid) probability that a collision involving a downwind mean-sized dune will have a mass ratio $r > r_*$ and thus result in two similarly sized dunes.

Table 1
Table showing the probability that a collision involving a mean-sized influx dune will yield more similarly-sized dunes, for simulations with different influx ranges, and at the lowest r_* yielding runaway growth.

Dune size range [m^2]	Mean size (M)	Threshold r_*	Probability at threshold r_* (%)
10–70	40	0.4	90
25–55	40	0.6	100
35–45	40	0.9	90
25–175	100	0.4	90
50–150	100	0.5	100
80–120	100	0.8	100

If the dune range given is $c-d$, then the mean size $M=(c+d)/2$, and the probability $P(a>Mr^*)=1-P(a<Mr^*)=1-(Mr^*-c)/(d-c)=\left(M-Mr^*+\sqrt{3}\sigma/\sigma\sqrt{12}\right)$.

We hypothesize that calculating the probability that $a>r_*M$ for the lowest r_* which yields runaway growth will yield insight about the boundary between the possible simulation end states. The results of many simulations are shown in Table 1, where it can be seen that the probability at the boundary between the two end states is consistently very large. We can see in Fig. 16 that as long as the size distribution of the influx dunes is not overly wide ($\sigma<0.5M$), even with a 90% probability that any single interaction will involve a mass ratio $r>r_*$ and will yield more similarly-sized dunes, the simulation will still achieve runaway growth.

Physical implications of this probabilistic analysis are discussed in Section 5.1.

4.6. Comparison with prior study

The study done by Lee et al. (2005) utilized the interaction function $f(r)=1.3\sqrt{r-\gamma}$, with the range constrained to be real and in [0,1], where γ (which is related to r_*) was treated as a free parameter. In this study, semi-infinite boundaries were used with a temporary influx: the influx was set to zero after 100 dunes were injected. The number of remaining dunes in the system, once the system was size-sorted, can be examined as a measure of coalescence. If coalescence occurs (and the number of dunes decreases), then a runaway end state would be likely if the influx had not been turned off. Conversely, if the system is to achieve a quasi-steady end state, then the total number of dunes should remain very close to 100.

Based on the influx dune distributions used in this study (uniform distributions of height with ranges 1–2 m or 1–10 m), it is possible to solve for the γ values such that a mean-sized influx dune will never grow larger after colliding with a smaller dune — for larger γ values, some collisions should result in coalescence. For the 1–2 m range (cross-sectional areas of 5.75–23 m^2), $\gamma=0.33$ ($r_*=0.44$), and for the 1–10 m range (5.75–575 m^2), $\gamma=0.032$ ($r_*=0.033$). As can be seen in Fig. 17, those γ values are where the final number of dunes deviates from 100 in their studies; i.e., those values correspond to where coalescence begins to occur.

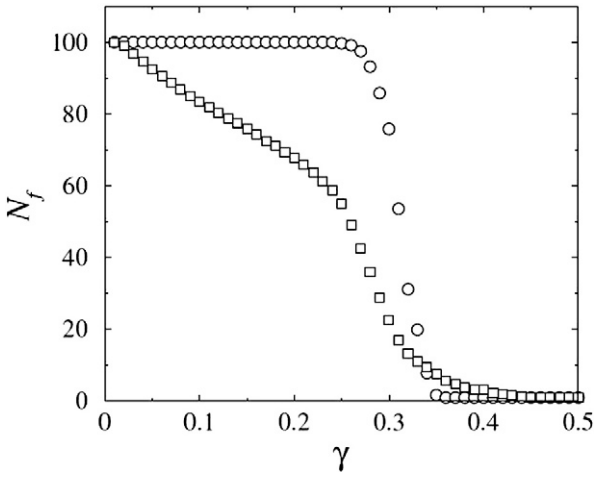

Fig. 17. This is Fig. 6 from Lee et al. (2005), showing the final number of dunes (N_f) as a function of γ, averaged over 1000 simulations. 100 dunes are injected, and then influx is set to zero. Injected dunes are randomly sized with heights between 1–2 m (circles) or 1–10 m (squares). The number of dunes decreases in time because of coalescence between dunes.

Table 2
A summary of different dune field model components, for a model with semi-infinite boundaries, and the effect each component has on the model's end state results.

Structural element		Effect
Interaction function	Form (e.g., steepness)	Timescale
	Extent of coalescence zone	Timescale
	Multiple regions of $f(r)>r$	Timescale
	Crossover value	End state
Initial conditions		Negligible as long as not containing dunes overly large compared to the influx, and sufficient time is given for them to be assimilated/run ahead
Influx condition	Mean value	Timescale
	Standard deviation/mean	End state

Any component which affects timescale will also affect dune size and spacing evolution. In this study, we were primarily interested in only the simulation's end state.

Although the differences in the influx condition (our influx is continuous) make it difficult to compare the results by Lee et al. (2005) with our results, this shows that the studies do not contradict each other.

5. Discussion

This study shows that whether or not a dune field model achieves a patterned structure depends intimately on the interaction dynamics and dune formation. Thus, both of these processes need to be well constrained before a model can be compared to a physical dune field. If one is only interested in predicting the end state of the simulation, however, just one parameter in dynamics (the interaction function crossover value) and one parameter in dune initialization (the influx condition's standard deviation/mean ratio) need to be constrained. Theoretically, if an actual dune field is patterned and appears to be stable, then finding one of these two parameters should also yield information about the other.

Many other structural factors do affect the timescale over which the simulation achieves its end state, however, which by extension affects dune size and interdune spacing (Table 2). This means that unless a physical dune field has achieved its end state, these other factors (such as dune velocity and initial conditions) must also be constrained to reliably compare simulation results with observations.

5.1. Implications

As was shown in Section 4.5, a dune field will achieve runaway growth even if a high probability (90%) exists that an average collision in the beginning of the dune field will result in similarly sized dunes ($r>r_*$). As an even larger probability is needed for the field to achieve a quasi-steady end state – which relates to a very careful coupling between the influx condition and the interaction function crossover value – it is surprising that most observed dune fields do not appear to be in a state of runaway growth.

Assuming the premise that the dune field model presented in Section 3 adequately captures the results of dune collisions, there are three extreme explanations:

1. Collisions are the dominant stabilizing mechanism for dune fields. Thus, for most dune fields to appear patterned, the physical system –

both the environmental conditions which influence dune formation and the interaction dynamics – must naturally fall into the small window needed for this to occur.
2. Collisions may play a role in redistributing sand from large dunes to small dunes, but the model is incomplete. Other processes (e.g., interdune sand flux or intrafield dune nucleation) or factors (e.g., variations in influx) are needed to increase the stability of patterned dune fields.
3. Patterned dune fields are not stable landforms. The timescale over which a dune field destabilizes, however, is very long compared to the timescales over which its environment changes.

The first point is a plausible explanation for barchan fields, as numerical simulations of barchan dune interactions yield interaction functions with very low crossover values, which means the influx distribution does not need to be tightly constrained for the dune field to possibly become patterned. For example, Durán et al. (2005) found an $r_* \sim 0.12$ (volume ratio) for zero-offset collisions between barchans (Fig. 6). Using a crossover value that low in this model (translated to $r_* = 0.16$ for the cross-sectional area ratio by Lee et al. (2005)), and assuming a uniformly distributed area influx starting with 10 m^2 (~1 m height), the upper limit on the influx distribution can be as high as 110 m^2 (~5 m height) and the system will still achieve a quasi-steady state. Additionally, even if the crossover value is higher, it seems reasonable to assume that dune initialization should result in a narrow range of dune sizes, so still yield a quasi-steady end state.

We showed (Section 2.3), however, that simulations of transverse dune collisions yield $r_* = 1$. In this case, if transverse dune fields do achieve stable patterned structures, the second explanation must be correct. Alternatively, the third point is correct (or the original premise is wrong).

The second explanation (that the model is incomplete) needs to be carefully evaluated, as size- or age-dependent dune field stabilizing processes do occur. For example, large barchan dunes can be destabilized through wind variations and dune collisions, as long-wavelength perturbations form on the flanks of these dunes and break away. This prevents any dunes from becoming overly large and increases the likelihood that a dune field will remain patterned. Intrafield dune destabilization has been studied in the field (Elbelrhiti et al., 2005; Gay, 1999), in the laboratory (Endo et al., 2004), and in three-dimensional continuum simulations (Durán et al., 2005; Katsuki et al., 2005; Elbelrhiti et al., 2008).

The results of dune collisions may also depend on local conditions, such as the age of dunes involved or the type of sand making up the dunes. In Besler (2002), on-going dune collisions were studied in different fields in the Libyan desert, and the apparent collision results in each locale were compared with the dunes' granulometrics. In that study, it was hypothesized that a downwind dune made of softer and finer grains was more likely to coalesce with the colliding upwind dune, while a downwind dune made of more compacted and coarser grains was more likely to have a collision result in ejection. As younger/smaller dunes are more likely to contain softer, finer grains, and older/larger dunes are more likely to contain more compacted, coarser grains (Besler, 2005), this would mean that large dunes would be less likely to coalesce and enter runaway growth.

The rate of sand redistribution through these processes and/or their effect on the dune field's interaction function, however, still needs to be quantified through numerical simulation, observation, and/or laboratory experiments, before these processes can be included in a dune field model.

The final explanation is in reference to the fact that, in this model, the timescale of collisions was ignored and the rate of migration and dune injection were arbitrarily specified. This is acceptable as long as we are concerned only with the dune field's end state. However, if the timescale over which a dune field achieves runaway growth is overly long, environmental conditions may vary or the dune field may run into a physical boundary long before the dune field will reach this state. Currently, there is no reason to expect that the timescale over which runaway growth occurs should be very long. In this study, our choice of parameters yielded timescales on the order of a century (which is consistent with estimates by Hersen et al. (2004)).

However, long timescales may play a role if the actual distribution of dune sizes is strongly-peaked. With simulations that were run with Gaussian influx dune size distributions (with comparable σ/M as were used with uniform distributions, and with a low-end cutoff at 1 m^2), runaway growth occurred at lower crossover values (Fig. 18), but after much longer time periods (10–100 times longer). This was unexpected, because we had hypothesized that a peaked distribution could have the same standard deviation/mean ratio value as a uniform distribution, and be far less likely to have a sufficient number of small r interactions for the dune field to achieve runaway. The 'tails' of the distribution ended up being more influential than the peak, however — very large or very small dunes had a very low probability of being injected into the dune field, but after a very long time it was more likely that an apparently 'stable' patterned dune field would become destabilized and enter runaway growth.

The peaked nature of the distribution did exert a 'stabilizing' influence on transitory dune field dynamics — in a few cases with intermediary r_* values, a field would appear to switch from quasi-steady state to runaway growth and then back. Additionally, when simulations were run with tail-less Gaussian distributions (which is a more physically realistic distribution), the observed decrease in the threshold crossover values disappeared. The impact of using a realistic influx dune size distribution should be more thoroughly studied in the future.

5.2. Possible future model improvements

As discussed in the second point in Section 5.1, some additional physical processes may need to be included before the model can provide a sufficiently complete picture of dune field evolution. For example, the model may be improved by including (i) sand flux between and during collisions, (ii) dune destabilization between and during collisions, and (iii) variations in the influx condition or

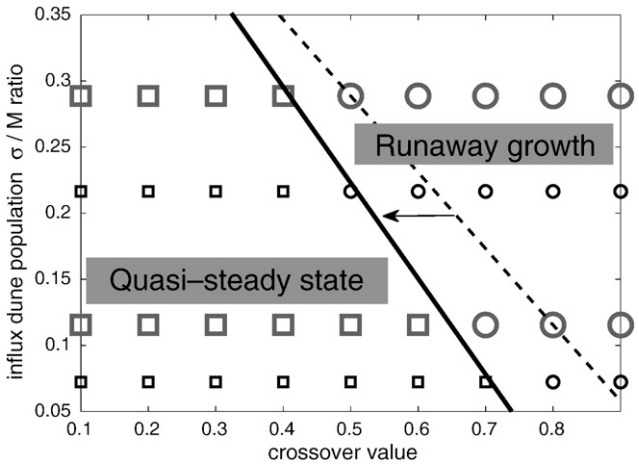

Fig. 18. Plot showing the model end state, as a function of the interaction function crossover value and the standard deviation/mean ratio (Gaussian distribution). Notice that the boundary between the regions corresponding to each end state (roughly demarked by the solid trendline): quasi-steady state (squares) vs. runaway growth (circles), is at lower crossover values as compared to the results with uniform distribution (dashed trendline). However, simulations required 10–100x longer times to achieve an end state. Additionally, the left shift in the boundary disappears if the tails are removed from the Gaussian distribution. As in Fig. 16, the size of the point-markers denotes the mean of the dune size distribution.

interaction function. Additionally, if the model is to be expanded to consider evolution of a three dimensional dune field, dunes should be able to split into more than two dunes after a collision (Durán et al., 2005; Katsuki et al., 2005).

As long as the processes and effects considered are assumed to occur during a collision (such as sand flux, dune destabilization, and/or a higher number of resultant dunes), then the model would not need to significantly change in structure. The effects of sand flux and dune destabilization during a collision could simply be added into a higher-dimension interaction function (e.g., the total size of the dunes and the size ratio after collision could be a function of the size ratio and total sizes of the dunes before collision), and the interaction function could reflect the formation of more than two dunes by calculating multiple after-collision size ratios. Thus, although the function would doubtlessly be much more complex, it is unlikely that the nature of its effect on the dune field's end state would significantly change from what is presented in this study; i.e., it is likely that the "crossover surface" would still be the only influential component of the interaction function in the analysis about the end state of a dune field.

Another possible addition to the model would be to include temporal or spatial variations in the interaction function (e.g., because of granulometric sand type changes in the dunes (Besler, 2002)), or temporal variations in the influx condition (e.g., because of changes in local vegetation or sand supply). In this case, the range of possible r_* and/or σ/M values, and the rates of parameter change would need to be incorporated into the analysis, as those factors could push a dune field between end states. For example, if the interaction function crossover value could widely vary over short time/spatial scales, a dune field that would be expected to enter runaway growth at the mean crossover value could in fact be stabilized as large dunes would break up before becoming sufficiently larger than the surrounding dunes. If, instead, the influx dune population's standard deviation changed over long time periods, an apparently patterned dune field could be destabilized.

Furthermore, if the variation in range and period of these parameters were properly coupled, it should be possible to see oscillation between the two end states. In fact, all of these different types of behavior (apparently runaway → patterned, apparently patterned → runaway, and oscillatory) have been observed in simulations with a Gaussian distribution of influx sand dunes (see Section 5.1).

To complete the model, it may also be necessary to allow dune evolution between collisions — such as through sand flux or dune destabilization. These types of inter-collision processes, however, would be more problematic to add into the model, as now dune evolution is partially uncoupled from the collisions. New analysis would need to be completed, carefully combining inter- and intra-collision functions, and additional influential parameter(s) from the inter-collision processes would need to be identified.

Finally, if we are to include temporally or spatially varying parameters, and/or inter-collision dune evolution in the model, then timescale becomes an important concern. Now dune evolution can occur continuously (e.g., through intra- and inter-collision sand flux), semi-periodically (e.g., with a varying influx condition), or stochastically (e.g., storm-caused destabilization of large dunes). With these different timescales, superimposed periodicities between dune growth and destabilization may occur, possibly resulting in pseudo-periodic or chaotic switching between the runaway growth and quasi-steady states.

As we can see, a more "complete" model can quickly become much more complex — and interesting. However, to properly include these processes in the model, identify influential parameters, and be able to derive predictions about a particular dune field, a far better understanding of these processes is needed. Thus, experimental and field work is vital in providing a quantification of the timescales and effects these different processes have on dune and dune field evolution.

6. Conclusion

In this study, we demonstrated that a profound difference exists between modeling a large field using periodic or semi-infinite domains. The evolution of dune size and spacing differs depending on the boundary conditions used. Thus, if one is interested in looking at trends in dune size or spacing, justification must be given for the boundary conditions chosen. However, although dynamically very different, both periodic and semi-infinite boundaries yield the same end state for the same crossover values.

If the model has semi-infinite boundary conditions, then initial conditions appear to be unimportant as long as the initial dunes are not substantially larger than the influx dunes, and as long as sufficient time is given for the initial dunes to assimilate with the influx dunes or run out ahead of the rest of the dune field.

We found that the influx condition has a significant effect on the results of a simulation. Only the standard deviation/mean ratio of the influx size distribution, however, affects the end state of the dune field. The mean size of the influx dune also affects the mean dune size and spacing, if the system achieves a quasi-steady end state.

We also found that in specifying the interaction function used to dictate the results of dune collisions, the exact functional form is not important as long as only the end state is of interest — the crossover value is the only important parameter within the interaction function.

Thus, assuming this multiscale approach is valid, field and laboratory studies are needed to provide estimates of the *influx dune size distribution standard deviation/mean ratio* (σ/M)and *interaction function crossover value* (r_*) for actual dune fields. If it proves possible to tightly constrain those two parameters for a specific dune field, then this study shows that we can make reliable predictions about that dune field's end state. Alternatively, if the actual dune field's end state is known, we can derive information about the dynamics and environment of the dune field.

Acknowledgements

SD was supported by a NASA Harriet G. Jenkins Predoctoral Fellowship. KG was supported in part by NSF award DMS-0405596. The hours of help provided by B. Jackson, and J. Kao in discussion and editing assistance are also gratefully acknowledged.

Appendix A

Here we present the equations and variables used in our dune model (previously described in Section 2.1). In our model, we use linearized dune model equations, similar to those presented in Andreotti et al. (2002b):

1. The profile of the near-surface airflow ($s(x,t)$) is a function of topography ($h(x,t)$). To account for airflow separation in the lee of dune crests, our separation bubble follows the portion of an ellipse extending downwind with an aspect ratio of 6, with continuity in both position and slope at the dune's crest (Schatz and Herrmann, 2005). On the stoss slopes of dunes and downwind of the point that the separation bubble re-intersections with the topography, the "separation bubble" follows the topography ($s = h$).
2. The shear stress (τ) is the far-field amount (τ_0) modified by a topography-induced pertubation ($\tilde{\tau}$).

$$\tau(x,t) = \tau_0(1 + \tilde{\tau}(x,t)). \quad (A-1)$$

Local wind conditions set τ_0 (via the Prandtl–von Kármán relation), and $\tilde{\tau}$ is calculated via the Jackson–Hunt equation (Jackson and Hunt, 1975):

$$\tilde{\tau}(x,t) = A \int_{\text{simulation domain}} s_x(y,t)/(\pi(x-y))\mathrm{d}y + Bs_x(x,t), \quad (A-2)$$

where A and B are dimensionless parameters that depend on the logarithm of the ratio between the geometric scale and the surface roughness (Kroy et al., 2002); for typical aeolian dune sizes, $A \sim 4$, $B \sim 1$. In the shadow zones, where air recirculation is too weak to induce saltation, $\tau = 0$.

3. The saturated sand flux (q_s) has been empirically measured to be $\sim\tau^{3/2}$ (Bagnold, 1941). In this model, a linearized version of that relation is used:

$$q_s(x,t) = Q(1 + 3\tilde{\tau}(x,t)/2), \tag{A-3}$$

where Q is the far-field saturated sand flux ($\sim\tau_0^{3/2}$). The actual sand flux (q) is then found by integrating the following equation:

$$q_x(x,t) = \begin{cases} \max(((q_s(x,t) - q(x,t))/L_s, 0), & \text{in shadow zones } (s<h), \text{ deposition only} \\ 0, & \text{over bedrock } (h<\varepsilon \text{ and } s = h), \\ & \text{no erosion/deposition} \\ (q_s(x) - q(x))/L_s, & \text{otherwise} \end{cases} \tag{A-4}$$

where L_s is the spatial delay of the evolution of the saltation layer towards q_s and ε is the sand height at which it is assumed there is no sand to erode (arbitrarily chosen to be a few sand grain diameters). The parameter L_s is the dune model's characteristic length scale and depends on environmental parameters such as grain size/density and fluid density (Claudin and Andreotti, 2006; Parteli and Herrmann, 2007). In this study of terrestrial aeolian dunes, $L_s \sim 1$ m.

The dune topography changes via mass conservation with the sand flux. Additionally, avalanches are accounted for via a diffusion term:

$$h_t = -q_x/\phi + (D(h_x)h_x))_x, \tag{A-5}$$

where ϕ is the volume correction for piled sand vs. bulk sand ($\rho_{dune}\rho_{sand} \sim 0.6$) and the values of D were chosen to reflect the instantaneous nature of avalanches when the slope exceeds the angle of repose, and the weak influence of diffusion when the slope is less than the angle of repose:

$$D(h_x) \sim \begin{cases} 10^{-3}, & |h_x| < \tan(34^\circ) \\ 1, & |h_x| \geq \tan(34^\circ). \end{cases} \tag{A-6}$$

We note that these equations can be non-dimensionalized by rescaling length in terms of L_s and time in terms of Q/L_s^2. This allows for comparison between dunes forming in different environments: terrestrial aeolian or subaqueous dunes, or aeolian dunes on Mars, Titan or Venus (Andreotti et al., 2002b; Claudin and Andreotti, 2006; Parteli and Herrmann, 2007). In this study, as the dune size ratio before and after collisions were the only dune model results transferred into the dune field model, the specific physical scales considered are irrelevant.

References

Andreotti, B., Claudin, P., Douady, S., 2002a. Selection of dune shapes and velocities, Part 1: dynamics of sand, wind, and barchans. The European Physical Journal B 28, 321–339.

Andreotti, B., Claudin, P., Douady, S., 2002b. Selection of dune shapes and velocities, Part 2: a two-dimensional modeling. The European Physical Journal B 28, 341-325.

Bagnold, R.A., 1941. The Physics of Blown Sand and Desert Dunes. Methuen.

Besler, H., 2002. Complex barchans in the Libyan Desert: dune traps or overtaking solitons? Zeitschrift für Geomorphologie N. F. Supplementband 126, 59–74. Mar.

Besler, H., 2005. The granulometric evolution of aeolian sands — an empirical and statistical approach. In: Garcia-Rojo, R., Hermann, H.J., McNamara, S. (Eds.), Powders and Grains, pp. 973–976.

Bishop, M.A., 2007. Point pattern analysis of north polar crescentic dunes, Mars: a geography of dune self-organization. Icarus 191, 151–157.

Bourke, M.C., Balme, M., 2008. Megabarchans on Mars. Planetary Dunes Workshop: a Record of Climate Change, held April 29–May 2, 2008 in Alamogordo, New Mexico. LPI Contribution No. 1403, pp. 17–18.

Claudin, P., Andreotti, B., 2006. A scaling law for aeolian dunes on Mars, Venus, Earth, and for subaqueous ripples. Earth and Planetary Science Letters 252, 30–44. Nov.

Durán, O., Schwämmle, V., Herrmann, H.J., 2005. Breeding and solitary wave behavior of dunes. Physical Review E 72 (2), 021308. Aug.

Elbelrhiti, H., Claudin, P., Andreotti, B., 2005. Field evidence for surface-wave-induced instability of sand dunes. Nature 437, 720–723.

Elbelrhiti, H., Andreotti, B., Claudin, P., 2008. Barchan dune corridors: field characterization and investigation of control parameters. Journal of Geophysical Research 113, F02S15.

Endo, N., Taniguchi, K., Katsuki, A., 2004. Observation of the whole process of interaction between barchans by flume experiments. Geophysical Research Letters 31, L12503.

Gay, S.P., 1999. Observations regarding the movement of barchan sand dunes in the Nazca to Tanaca area of southern Peru. Geomorphology 27, 279–293. Mar.

Herrmann, H.J., Sauermann, G., Schwämmle, V., 2005. The morphology of dunes. Physica A 358, 30–38.

Herrmann, H.J., Durán, O., Parteli, E.J.R., Schatz, V., 2008. Vegetation and induration as sand dunes stabilizators. Journal of Coastal Research 24 (6), 1357–1368.

Hersen, P., 2004. On the crescentic shape of barchan dunes. European Physical Journal B 37, 507–514.

Hersen, P., Douady, S., 2005. Collision of barchan dunes as a mechanism of size regulation. Geophysical Research Letters 32, L21403.

Hersen, P., Andersen, K.H., Elbelrhiti, H., Andreotti, B., Claudin, P., Douady, S., 2004. Corridors of barchan dunes: stability and size selection. Physical Review E 69 (1), 011304. Jan.

Jackson, P.S., Hunt, J.C.R., 1975. Turbulent wind flow over a low hill. Quarterly Journal of the Royal Meteorological Society 101 (430), 929–955.

Katsuki, A., Nishimori, H., Endo, N., Taniguchi, K., 2005. Collision dynamics of two barchan dunes simulated using a simple model. Journal of the Physical Society of Japan 74 (2), 538–541. Feb.

Kocurek, G., Ewing, R.C., 2005. Aeolian dune field self-organization — implications for the formation of simple versus complex dune-field patterns. Geomorphology 72, 94–105.

Kroy, K., Sauermann, G., Herrmann, H.J., 2002. Minimal model for aeolian sand dunes. Physical Review E 66 (3), 031302 Sep.

Lee, J.H., Sousa, A.O., Parteli, E.J.R., Herrmann, H.J., 2005. Modelling formation and evolution of transverse dune fields. International Journal of Modern Physics C 16 (12), 1879–1892.

Lima, A.R., Sauermann, G., Herrmann, H.J., Kroy, K., 2002. Modelling a dune field. Physica A 310, 487–500.

Livingstone, I., Wiggs, G.F.S., Baddock, M., 2005. Barchan dunes: why they cannot be treated as 'solitons' or 'solitary waves'. Earth Surface Processes and Landforms 30, 255–257.

Parteli, E., Herrmann, H.J., 2003. A simple model for a tranverse dune field. Physica A 327, 554–562.

Parteli, E.J., Herrmann, H.J., 2007. Dune formation on the present Mars. Physical Review E 76, 041307.

Parteli, E.J.R., Durán, O., Herrmann, H.J., 2006a. The shape of the barchan dunes in the Arkhangelsky Crater on Mars. In: Mackwell, S., Stansbery, E. (Eds.), 37th Annual Lunar and Planetary Science Conference. Lunar and Planetary Inst. Technical Report, vol. 37, p. 1827. Mar.

Parteli, E.J.R., Schwämmle, V., Herrmann, H.J., Monteiro, L.H.U., Maia, L.P., 2006b. Profile measurement and simulation of a transverse dune field in the Lençóis Maranheses. Geomorphology 81, 29–42.

Sauermann, G., Kroy, K., Herrmann, H.J., 2001. Continuum saltation model for sand dunes. Physical Review E 64 (3), 031305. Sep.

Sauermann, G., Andrade Jr., J.S., Maia, L.P., Costa, U.M.S., Araùjo, A.D., Herrmann, H.J., 2003. Wind velocity and sand transport on a barchan dune. Geomorphology 1325, 1–11.

Schatz, V., Herrmann, H.J., 2005. Flow separation in the lee side of transverse dunes. In: Garcia-Rojo, R., Herrmann, H.J., McNamara, S. (Eds.), Proceedings of Powders and Grains, pp. 959–962.

Stam, J.M.T., 1996. Migration and growth of aeolian bedforms. Mathematical Geology 28, 519–536.

Werner, B.T., 1995. Eolian dunes: computer simulations and attractor interpretation. Geology 23, 1107–1110.